1412–1418 *Nucleic Acids Research, 1997, Vol. 25, No. 7*

The effect of ionic conditions on DNA helical repeat, effective diameter and free energy of supercoiling

Valentin V. Rybenkov, Alexander V. Vologodskii[1] and Nicholas R. Cozzarelli*

Department of Molecular and Cell Biology, University of California, Berkeley, CA 94720, USA and [1]Department of Chemistry, New York University, New York, NY 10003, USA

Received November 21, 1995; Revised and Accepted February 13, 1997

ABSTRACT

We determined the free energy of DNA supercoiling as a function of the concentration of magnesium and sodium chloride in solution by measuring the variance of the equilibrium distribution of DNA linking number, $\langle(\Delta Lk)^2\rangle$. We found that the free energy of supercoiling changed >1.5-fold over the range of ionic conditions studied. Comparison of the experimental results with those of computer simulations showed that the ionic condition dependence of $\langle(\Delta Lk)^2\rangle$ is due mostly to the change in DNA effective diameter, *d*, a parameter characterizing the electrostatic interaction of DNA segments. To make this comparison we determined values of *d* under all ionic conditions studied by measuring the probability of knot formation during random cyclization of linear DNA molecules. From the topoisomer distributions we could also determine the changes in DNA helical repeat, γ, in mixed NaCl/$MgCl_2$ solutions. Both γ and *d* exhibited a complex pattern of changes with changing ionic conditions, which can be described in terms of competition between magnesium and sodium ions for binding to DNA.

INTRODUCTION

Recent theoretical and experimental studies have shown that the conformational properties of supercoiled DNA strongly depend on ionic conditions (1–5). Computer simulations also predict that variations in ionic conditions should cause significant changes in the free energy of supercoiling (1,6). Analysis of many properties of supercoiled DNA requires knowledge of the dependence of supercoiling free energy, *G*, on superhelix density, σ. $G(\sigma)$ is particularly important for the theoretical treatment of non-canonical structures in supercoiled DNA (reviewed in 7). Experiments with supercoiled DNA are carried out under various ionic conditions and thus we investigated how $G(\sigma)$ depends on these conditions.

Our approach is based on measurements of the equilibrium distribution of DNA linking number, *Lk*. Since 1975, when the laboratories of Wang and Vinograd published their elegant determinations of the distributions and their use to obtain $G(\sigma)$ (8,9), the method has been applied to various solution conditions and DNA lengths (10–13). Many theoretical studies have also analyzed the distributions (14–20). In this work we systematically measured the dependence of the variance of the topoisomer distribution on the concentrations of NaCl and $MgCl_2$ in solution and found that the variance changes significantly.

To compare the experimental data with the results of computer simulations we had to know the values of the DNA effective diameter, *d*, under the ionic conditions used. This parameter characterizes the electrostatic interactions between DNA segments (21,22) and corresponds to the diameter of an uncharged model chain that mimics the conformational distribution of an actual DNA molecule. The values of *d* are known for solutions containing NaCl or $MgCl_2$ alone (21,23–26) and we determined the effective diameter for mixtures of both salts. We calculated *d* from the probability of knots in cyclized DNA (25,26).

Analysis of the equilibrium topoisomer distributions allowed us to determine another feature of supercoiled DNA. Changes in solution conditions also affect the DNA helical repeat, the number of base pairs per turn, γ. We systematically measured changes in DNA helical repeat in mixed solutions of NaCl and $MgCl_2$. These results, together with the data on DNA effective diameter obtained for the same ionic conditions, extend our understanding of competition between sodium and magnesium ions for binding to DNA.

MATERIALS AND METHODS

The 7.02 kb plasmid pAB4 (27) was purified by the Triton lysis method (28). It was singly nicked by limited digestion with DNase I in the presence of ethidium bromide (29) and purified by extraction with phenol, phenol/chloroform and chloroform, followed by ethanol precipitation. For $MgCl_2$-containing solutions, we prepared equilibrium topoisomer distributions by ligation of singly nicked DNA circles with T4 DNA ligase. The ligation reactions were incubated for 4 h in the presence of 0.5 mM sodium phosphate, pH 7.5, 5 μg/ml DNA, 0.1 mM ATP and the indicated amounts of NaCl, $MgCl_2$ and spermidine·3HCl. The amount of ligase (2 Weiss U/ml) was 100-fold lower than the concentration found to disturb the DNA conformational equilibrium (30). For 0.03–0.2 M NaCl solutions (lacking $MgCl_2$) we relaxed supercoiled DNA with wheat germ topoisomerase I (topo I), purified as described (31). The relaxation reactions contained 0.5 mM sodium phosphate, pH 7.5, 0.2 mM EDTA, the

* To whom correspondence should be addressed. Fax: +1 510 643 1079; Email: cozzlab@mendel.berkeley.edu

indicated amounts of NaCl, 1 μg DNA and 3–100 U topo I (0.3–10 molar ratio of enzyme to DNA) in 30 μl. There was always a range of topo I concentrations which yielded the same distribution. At lower enzyme concentrations, relaxation was incomplete and stoichiometric amounts of topo I widened the distributions. Control experiments showed that in the presence of $MgCl_2$ these plateau values for the distributions were identical to those obtained by ligation of nicked circular DNA (data not shown). Therefore, these distributions are at equilibrium.

Both ligation and relaxation reactions were carried out at 30 ± 1°C and were quenched by extraction with phenol/chloroform. After extraction with chloroform and ethanol precipitation, the DNA was resolved by gel electrophoresis (1.0% agarose gel, 1.2 V/cm for 64 h) in TAE buffer supplemented with 0.4 μg/ml chloroquine. The DNA was detected by Southern hybridization and quantified using a PhosphorImager (Molecular Dynamics).

Two-dimensional gel electrophoresis

Wheat germ topo I has little activity at NaCl concentrations <0.03 M. Therefore, to determine the change in DNA helical repeat at low salt concentrations, we measured the shift of the topoisomer distribution prepared by ligation in the presence of 0.01 M NaCl and 20 mM $MgCl_2$ upon transfer of the DNA to a low salt electrophoretic buffer, the buffer in the first dimension of a two-dimensional (2D) electrophoresis. The buffer for the second dimension contained chloroquine to unambiguously resolve all topoisomers (10,32). The method is based on the expectation that at low superhelical density the electrophoretic mobility of closed circular DNA depends on the absolute value of linking number difference, $|\Delta Lk|$. Therefore, comparison of the mobilities of several consecutive topoisomers allows the determination of ΔLk for each topoisomer during electrophoresis in the first dimension. For example, if two consecutive topoisomers have identical mobilities in the first dimension their ΔLk equals +0.5 and –0.5. If no two topoisomers have equal mobilities in the first dimension a more sophisticated analysis, outlined below, is needed. Because the position of the center of the distribution can also be found from the analysis of band intensities (see equation 2 in Results), the method allows direct measurement of the change in ΔLk value caused by the change in ionic conditions.

We prepared an equilibrium distribution of topoisomers by ligating singly nicked circular DNA in 0.01 M NaCl, 20 mM $MgCl_2$ and 0.1 mM ATP. To ensure that both positively and negatively supercoiled topoisomers could be detected on a gel (Fig. 1), we mixed this DNA with DNA ligated in the presence of ethidium bromide. Electrophoresis in the first dimension was under the ionic conditions of interest and the second in TAE buffer supplemented with chloroquine. The sign of topoisomers in Figure 1 denotes whether they were positively or negatively supercoiled during electrophoresis in the first dimension. If the distance migrated by each topoisomer in the first dimension, x_i, depends linearly on the absolute value of ΔLk under the conditions of electrophoresis, the ΔLk value of the jth topoisomer (ΔLk_j) is

$$\Delta Lk_j = 0.5\frac{x_j - x_i}{x_{i-1} - x_i} + 0.5(j - i), \qquad \mathbf{1}$$

where j is a positive topoisomer and i and $i - 1$ are negatively supercoiled. In our experiments, mobility was linearly dependent on ΔLk only for topoisomers –4 to –1 and 2 to 5. Thus, for the gel

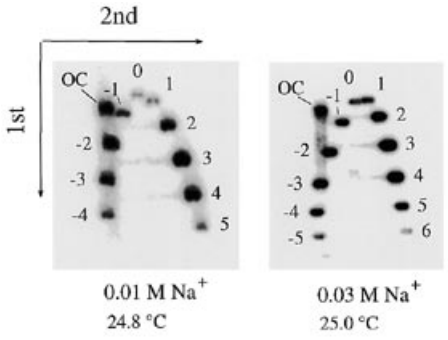

Figure 1. Measurement of the linking number difference by 2D gel electrophoresis. An equilibrium distribution of topoisomers was prepared by ligating nicked circular DNA in 0.01 M NaCl and 20 mM $MgCl_2$ at 24.8°C and resolved by 2D gel electrophoresis as described in Materials and Methods. To ensure that both positive and negative topoisomers could be detected on the gel, the distribution was mixed with another, negatively supercoiled distribution obtained by ligating nicked circular DNA in the presence of ethidium bromide. The directions of the first and second dimensions are indicated by arrows. During electrophoresis in the first direction, topoisomers numbered 1 to 6 were positively supercoiled and topoisomers –5 to 0 were negatively supercoiled. Assuming that the mobilities of negative and positive topoisomers depend only on the absolute value of their linking number difference, $|\Delta Lk|$, comparison of the vertical positions of positive and negative topoisomers allows the determination of ΔLk for each topoisomer. The average temperature of the gels during electrophoresis in the first dimension is also shown. The center of our reference distribution (0.01 M NaCl, 20 mM $MgCl_2$) has a ΔLk of +3.2 relative to the topoisomer denoted 0. OC, open circular DNA.

in Figure 1 we chose $j = 3$ and $i = -2$. This procedure allowed the determination of ΔLk with an accuracy of about ±0.1. We carried out measurements for the same mixture of topoisomers but with NaCl concentrations of 0.01, 0.03 or 0.075 M.

For better resolution during gel electrophoresis, we used the smaller 2.95 kb pUCd2 plasmid for these experiments. The topoisomer distribution was resolved by electrophoresis through a 1.6% agarose gel in buffer containing 1 mM sodium phosphate, pH 7.5, 0.1 mM Na_3EDTA and 8 mM NaCl (10 mM Na^+ ions); 3 mM sodium phosphate, pH 7.5, 0.3 mM Na_3EDTA and 24 mM NaCl (30 mM Na^+ ions); 7.5 mM sodium phosphate, pH 7.5, 0.75 mM Na_3EDTA and 60 mM NaCl (75 mM Na^+ ions). The gels were run at 0.5 V/cm for 80 h with buffer recirculation and replenishment. The temperature of the gels was monitored during electrophoresis with a Fisherbrand NIST digital thermometer (Fisher Scientific) and the measured ΔLk values were corrected for temperature variation. For the second dimension, the gels were rotated by 90°, saturated for 3 h in TAE buffer supplemented with chloroquine and subjected to electrophoresis for 16 h at 1.2 V/cm. The DNA was detected by Southern hybridization and quantified using a PhosphorImager (Molecular Dynamics).

RESULTS

We used two methods to obtain an equilibrium distribution of DNA topoisomers. For $MgCl_2$-containing solutions we ligated nicked circular DNA with T4 DNA ligase, an enzyme which requires Mg^{2+}. For solutions in which NaCl was the only salt, we relaxed supercoiled DNA with wheat germ topo I. The distributions did not change if we used 3-fold higher or lower amounts of topo I, implying that the distributions obtained were at equilibrium. We resolved the resulting mixture by gel electro-

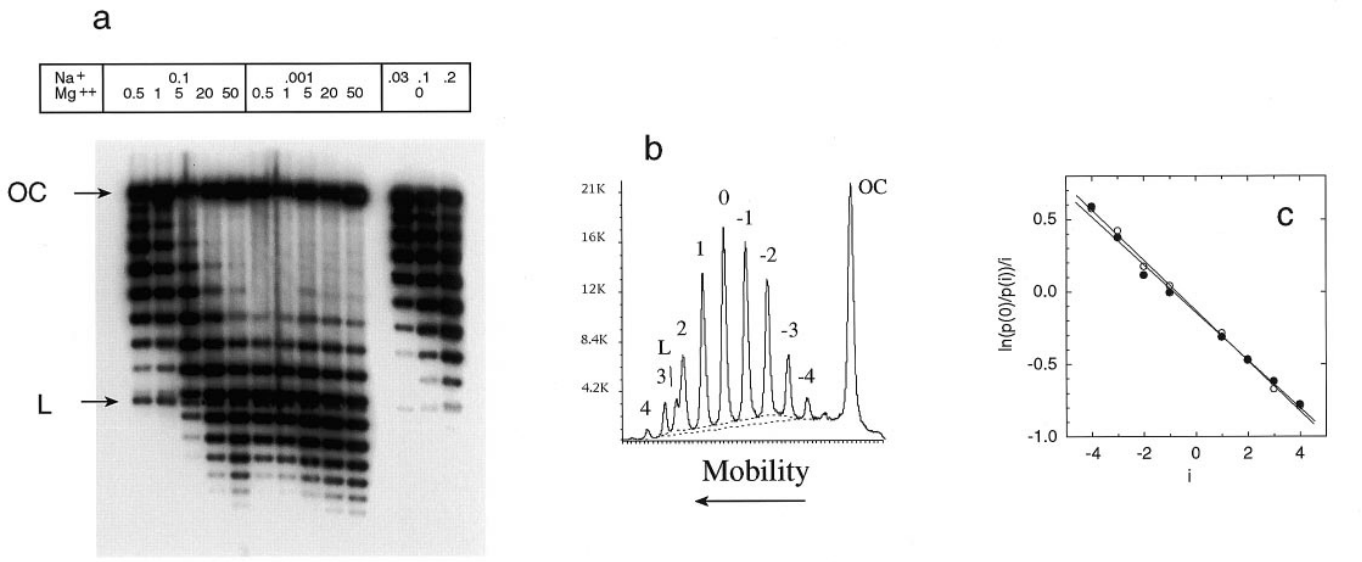

Figure 2. Quantitative analysis of the equilibrium topoisomer distribution. (**a**) Typical result of agarose gel electrophoresis showing the resolution of the equilibrium distributions of topoisomers generated under the indicated ionic conditions. OC, open circular DNA; L, linear DNA. The DNA in the gels was detected by Southern hybridization and quantified using a PhosphorImager. (**b**) A typical PhosphorImager scan of a sample from (a) ligated in 0.1 M NaCl and 5 mM $MgCl_2$. Dashed lines show limiting cases of baseline position used for the analysis. (**c**) Transformation of a Gaussian distribution of topoisomers to a linear form. Quantitation of the data for each of the baselines shown in (b) resulted in two sets of data which are shown with open and closed symbols. The lines correspond to linear regressions of the data. The slope of the line equals $1/[2\langle(\Delta Lk)^2\rangle]$ and its intercept with the *x*-axis equals -2δ (8). We averaged the results for the two positions of the baseline to obtain the values of $\langle(\Delta Lk)^2\rangle$ and δ. The standard deviation of the measured values of $\langle(\Delta Lk)^2\rangle$ was on average ±0.15.

phoresis and analyzed the distributions of topoisomers using a PhosphorImager. Typical topoisomer distributions are shown in Figure 2, together with a scan of a distribution in 0.1 M NaCl and 5 mM $MgCl_2$. The topoisomers on the gel are well separated, allowing for unambiguous measurement of the amount of DNA in each band.

It has been shown (8,9) that the equilibrium distribution of topoisomers is Gaussian. It is convenient for our analysis to present the distribution as

$$P(i) = A\exp\left[-\frac{(i-\delta)^2}{2<(\Delta Lk)^2>}\right], \qquad \mathbf{2}$$

where $P(i)$ is the amount of the ith topoisomer, $i-\delta$ is its linking number difference (also denoted ΔLk), $\langle(\Delta Lk)^2\rangle$ is the variance of distribution and A is a constant. Both the center and the width of the distribution can be found from its transformation to a linear form (8), as shown in Figure 2c.

The values of $\langle(\Delta Lk)^2\rangle$ for different ionic conditions are shown in Figure 3. Over the range of ionic conditions tested, the value of $\langle(\Delta Lk)^2\rangle$ changed >1.5-fold. When little or no $MgCl_2$ was present, the width of the topoisomer distribution increased with NaCl concentration. In solutions containing >5 mM $MgCl_2$, $\langle(\Delta Lk)^2\rangle$ was independent of NaCl concentration at the salt concentrations investigated.

Figure 3 shows the significant effect of ionic conditions on the value of $\langle(\Delta Lk)^2\rangle$. A large effect of $[Na^+]$ had been predicted by computer simulations (20). In the simulations, all changes of $\langle(\Delta Lk)^2\rangle$ were due to changes in DNA effective diameter, d. To quantitatively compare the experimental data with the theoretical predictions we had to determine the values of d for the ionic conditions used.

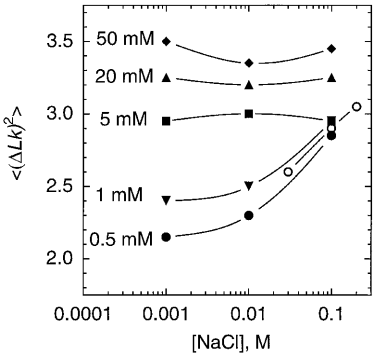

Figure 3. The variance of linking number difference in solutions containing both NaCl and $MgCl_2$. The values of $\langle(\Delta Lk)^2\rangle$ are plotted as a function of NaCl concentration. The solutions also contained 0.2 mM EDTA (●) or concentrations of $MgCl_2$ as indicated on the figure.

We calculated the values of d for different conditions from measurement of the probability of DNA trefoil knots, P_3, in a population produced by random cyclization of linear DNA. The value of P_3 greatly depends on the diameter of the polymer chain (25,33)

$$P_3 = P_0(L,a)\exp(-11 \times d/a) \qquad \mathbf{3a}$$

$$P_0(L,a) = 0.00122 \times L/a - 0.0132 \qquad \mathbf{3b}$$

where $P_0(L,a)$ is the knotting probability of a chain with zero diameter, L is the DNA contour length and a is the DNA persistence length. We considered the value of a to be constant and equal to 50 nm over the range of ionic conditions used (34).

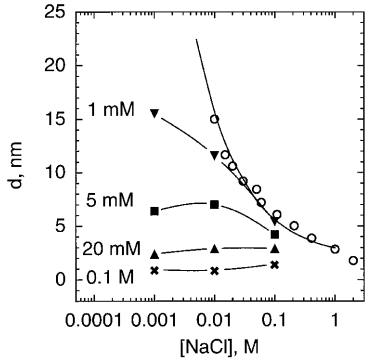

Figure 4. The DNA effective diameter as a function of NaCl and $MgCl_2$ concentration. The data corresponding to pure NaCl solutions (○) were taken from Rybenkov *et al.* (25) and are shown for comparison.

We measured the fraction of knotted molecules in 10 kb P4 DNA after its cyclization via its long cohesive ends. For this DNA and the chosen value of a, the value of $P_0(L,a) = 0.065$ (for details see 25). Comparison of the measured knotting probabilities with equation 3 allowed us to find the values of d (Fig. 4 and Table 1). The 10% standard deviation in the measured values of knotting probability resulted in an average uncertainty in the value of d of ±0.4 nm.

Table 1. Variation of DNA superhelical density, knotting probability, effective diameter and free energy of supercoiling in solutions containing NaCl, $MgCl_2$ and spermidine

$[Na^+]$ (M)	$[Mg^{2+}]$ (mM)	$[spermidine^{3+}]$ (mM)	$-100 \times \Delta\sigma$	$100 \times P_3$	d (nm)	K
0.001	0.5		0.80	ND	ND	1630
	1		0.80	0.21	15.6	1460
	5		0.81	1.6	6.4	1190
	20		0.86	3.8	2.4	1080
	50		0.90	4.9	1.3	1000
	100		ND	5.3	0.93	ND
0.01	0.5		0.59	0.46	12.0	1530
	1		0.64	0.51	11.6	1400
	5		0.74	1.4	7.0	1170
	20		0.83	3.4	2.9	1100
	50		0.90	5.0	1.2	1050
	100		ND	5.3	0.93	ND
0.1	0.5		0.04	ND	ND	1230
	1		0.10	2.0	5.4	1190
	5		0.40	2.6	4.2	1190
	20		0.67	3.4	2.9	1080
	50		0.85	4.1	2.1	1020
	100		ND	4.7	1.5	ND
0.02	10	0	0.76	2.1	5.1	1170
		1.5	0.55	3.6	2.7	1050
		3.0	0.44	6.0	0.36	920
		3.5	ND	6.8	–0.20	ND

ND, not determined.
The changes in DNA superhelical density are given relative to 0.1 M NaCl solution.

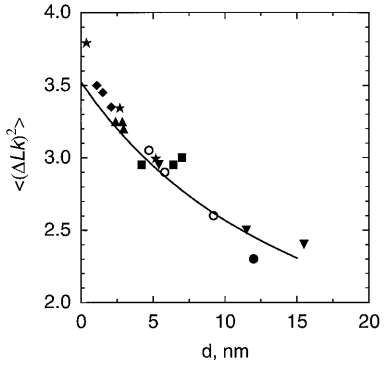

Figure 5. The variance in linking number as a function of DNA effective diameter. The measured variance in linking number [$\langle(\Delta Lk)^2\rangle$] from Figure 3 is plotted against the corresponding values of DNA effective diameter (d) from Figure 4. The symbols are as in Figure 3 except that stars (★) correspond to 10 mM sodium phosphate, pH 7.5, 10 mM $MgCl_2$ plus 0, 1.5 or 3 mM spermidine to give low values of d. The solid curve is the value of $\langle(\Delta Lk)^2\rangle$ calculated from equation 4.

The dependence of $\langle(\Delta Lk)^2\rangle$ on d for all mixtures of $MgCl_2$ and NaCl used and a comparison with the results of the theoretical analysis are collected in Figure 5. Several values for spermidine-containing solutions are also shown. Within the experimental accuracy, all the data points follow one smooth curve, even for solutions containing spermidine ions up to concentrations that promote DNA aggregation (35).

The solid line in Figure 5 is the theoretical dependence (20) calculated from the following equations

$$\langle(\Delta Lk)^2\rangle = \langle(Wr)^2\rangle + \langle(\Delta Tw)^2\rangle \quad \textbf{4a}$$

$$< (Wr)^2 > = \frac{< (Wr)^2 > 0}{1 + 2.75 \times d/a} \quad \textbf{4b}$$

$$< (\Delta Tw)^2 > = \frac{RTL}{4\pi^2 N_A C} \quad \textbf{4c}$$

Equation 4a represents $\langle(\Delta Lk)^2\rangle$ as the sum of the variances of twist, $\langle(\Delta Tw)^2\rangle$ and writhe, $\langle(Wr)^2\rangle$. Equation 4b interpolates the results of computer simulations for $\langle(Wr)^2\rangle$ as a function of d; the writhe of a polymer chain with a zero diameter, $\langle(Wr)^2\rangle_0$, is 2.69 for 7 kb DNA. Equation 4c specifies the dependence of $\langle(\Delta Tw)^2\rangle$ on DNA length, L, and on DNA torsional rigidity, C; R is the gas constant, N_A is Avogadro's constant and T is the absolute temperature. The dependence shown in Figure 5 used a value for C of 3×10^{-19} erg×cm, the value obtained from the topoisomer distribution of short DNA circles (11,12,17). Thus the only two parameters of the calculation, C and a, were taken from other studies rather than adjusted to fit the experimental data.

We conclude from Figure 5 that there is very good agreement between the theory and the experimental data. The agreement shows that change in DNA effective diameter is the major determinant in changes in $\langle(\Delta Lk)^2\rangle$. Variations with salt of DNA persistence length and torsional rigidity, if any, do not contribute significantly to the ionic condition dependence of $\langle(\Delta Lk)^2\rangle$. Note that very different concentrations of different ions can yield the same values of d. For example, the value of d is the same in 10 mM $MgCl_2$ as in 0.2 M NaCl. The Debye length, the characteristic length of electrostatic screening in a salt solution,

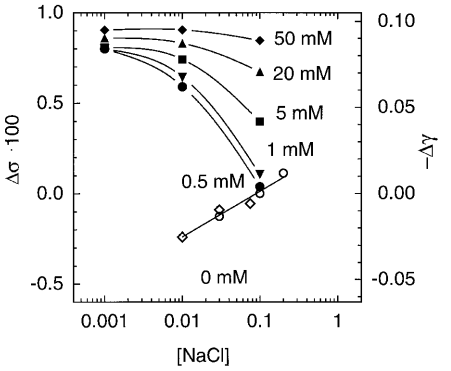

Figure 6. DNA superhelical density and helical repeat as a function of ionic conditions. The change in superhelical density, Δσ, and helical repeat, Δγ, upon transfer from a 0.1 M NaCl solution to the indicated mixtures of NaCl and $MgCl_2$ are shown. The curves indicate that DNA relaxed at 0.1 M NaCl will be negatively supercoiled in the tested $MgCl_2$ solutions. The symbols are as in Figure 3 except that the data shown with open diamonds (◊) were obtained by 2D gel analysis of topoisomer distributions and correspond to solutions containing no $MgCl_2$.

is 2.5-fold greater in 10 mM $MgCl_2$ than in 0.2 M NaCl. *d* is equal in these two salt solutions because the difference in Debye length is compensated for by a lower net linear charge density of DNA in $MgCl_2$ solutions. This conclusion fits with the 100-fold higher affinity of magnesium compared with sodium ions for DNA (36). The more efficient binding of magnesium ions lowers the value of the net DNA charge density. The competition between sodium and magnesium ions for binding to DNA is also responsible for the complex pattern of changes of DNA helical repeat in mixed NaCl/$MgCl_2$ solutions.

The shift of topoisomer distributions due to changes in ionic conditions, as in Figure 2a, can be described by the equation

$$\Delta Lk = Lk - N/\gamma \qquad \mathbf{5}$$

where *N* is the total number of base pairs in DNA and γ is the helical repeat of linear DNA under the given solution conditions. In closed circular DNA the change in γ shifts Δ*Lk* and, therefore, superhelical density, σ. The changes in σ (and γ) for different mixtures of NaCl and $MgCl_2$ are shown in Figure 6. In good quantitative agreement with previous data (37–39), the value of γ is lower in $MgCl_2$ than in NaCl solution. However, unlike previously reported results (39,40), we did not find any simple dependence of γ on $MgCl_2$ concentration. Instead, γ depends on the concentrations of both NaCl and $MgCl_2$. In solutions of 0.5–50 mM $MgCl_2$, the value of γ remains nearly the same. This means that binding of magnesium is already saturated at 0.5 mM $MgCl_2$. The dependence of γ on NaCl concentration is pronounced if the concentration of NaCl is much higher than that of $MgCl_2$. Therefore, the value of γ does not change significantly in the mixtures of 50 mM $MgCl_2$ and NaCl if the NaCl concentration does not exceed 0.1 M. On the other hand, γ decreases in mixtures of $MgCl_2$ and 0.1 M NaCl only when the $MgCl_2$ concentration is >1 mM.

Previously, the change in DNA helical repeat in NaCl solutions was measured at salt concentrations >0.05 M. To extend measurements to lower NaCl concentrations, we used 2D gel electrophoresis (10) to find the change in γ over the range 0.01–0.075 M NaCl. This method allows measurements at lower NaCl concentrations because it does not require enzymatic treatment of DNA under these conditions. Instead, an equilibrium distribution of topoisomers is prepared under conditions favorable for enzyme activity and the value of Δ*Lk* of the center of this distribution is measured under electrophoresis conditions of low NaCl concentration. We determined the mobility of the center of the equilibrium distribution of DNA topoisomers corresponding to 0.01 M NaCl, 20 mM $MgCl_2$ in a series of 2D gels (Fig. 1). In the first dimension, the gels were run under varying NaCl concentrations and the second dimension resolved topoisomers into distinct spots. The electrophoretic mobility of closed circular DNA depends only on the absolute value of Δ*Lk* and does not depend on its sign. Therefore, juxtaposition of the measured mobilities of positive and negative topoisomers allowed the determination of Δ*Lk* for all topoisomers under the conditions of the electrophoresis (see Materials and Methods for details). From the mobility of the center of the distribution (data not shown) we determined the change in Δ*Lk* caused by the change in ionic conditions. We validated the results of this method by comparing them with the results obtained by our basic enzymatic technique over the range 0.03–0.075 M NaCl. The two methods gave the same results for this overlapping range of NaCl concentration. Combining the data obtained by both methods (Fig. 6), we found that over the range 0.01–0.2 M NaCl the value of $d\sigma/d\log[NaCl]$ was equal to -0.0025 ± 0.0003.

DISCUSSION

Measurement of the variance of the equilibrium distribution of topoisomers has always been considered the most accurate way to determine the free energy of supercoiling, ΔG_{sc}. It was found (8,9) that

$$\Delta G_{sc} = \frac{KRT}{N}(\Delta Lk)^2 \qquad \mathbf{6}$$

where

$$K = \frac{N}{2 < (\Delta Lk)^2 >} \qquad \mathbf{7}$$

The value of *K* is independent of DNA length for molecules longer than 2.5 kb (8,9,11,12). It was generally accepted that for these DNA lengths the value of *K* is also independent of ionic conditions and equals 1100 ± 50. We found instead that *K* changes from 920 in a solution containing 3 mM spermidine to 1500 in 1 mM $MgCl_2$ (Table 1). This variation arises mostly from the change in electrostatic repulsion between DNA segments specified here by the DNA effective diameter (Fig. 5). Although changes in DNA bending and torsional rigidity can also contribute to the change in *K* (see equation 4), over the range of ionic conditions studied the net effects are too small to be measured by the technique used.

The changes in *K* with ionic conditions are especially important for studies of non-canonical DNA structures formed under superhelical stress (e.g. melted regions, cruciforms, Z-DNA segments and H-DNA), because their formation has been studied under various salt conditions. Estimations, however, of the energy parameters characterizing these structural transitions were always based on a *K* value of 1100 (see for example 41). For example, the energy parameters for Z-DNA formation were measured in TBE buffer (90 mM Tris-borate, 1 mM EDTA) (42–46). The value of *d* for this buffer is 13 nm (unpublished

data). It follows from Figure 5 that K equals 1450 rather than 1100 for this value of d.

We found that in the presence of 5–10 mM $MgCl_2$ the DNA effective diameter is nearly independent of the concentration of supplementing NaCl and is close to 5 nm. Thus, for a range of ionic conditions, including the physiological ones, the value of K equals ~1100, as was found before (8–10,12).

We measured the values of DNA effective diameter in mixtures of NaCl and $MgCl_2$ over a wide range of concentrations. The values of d found correspond to the DNA persistence length of 50 nm. For smaller values of a, the simulated dependence of P_3 on d becomes steeper. Yet, the values of d found are rather insensitive to uncertainty in the value of a. For a = 45 nm, for example, we would obtain d = 0.32 instead of –0.20 nm for 3.5 mM spermidine and 14.5 instead of 15.6 nm for 1 mM $MgCl_2$. The values of d in 100 mM $MgCl_2$ were <2 nm, the geometrical diameter of DNA. Such values of d reflect attraction between DNA segments at high $MgCl_2$ concentrations. Only in the presence of spermidine did we observe a knotting probability higher than the theoretical one for a chain with zero diameter (see equation 3). Such values were found previously by Shaw and Wang (26) for solutions containing >40 mM $MgCl_2$ and correspond to negative values of d. This discrepancy between the two studies may be due to experimental error, because the difference is only 4-fold larger than the standard deviation of our data.

The values of $\langle(\Delta Lk)^2\rangle$ have also been used a number of times to calculate DNA torsional rigidity (15–20,47). We found from our data that the value of C is equal to 2.7×10^{-19} erg×cm independent of ionic conditions. If a lower value of a is assumed in the simulations our data would yield higher values of C and for a = 45 nm we would obtain $C = 3.5 \times 10^{-19}$ erg×cm. However, the contribution of torsional fluctuations to the width of topoisomer distribution is relatively small, ~25%, for DNA longer than 2.5 kb. The rest of the variation arises from bending fluctuations of DNA. As a result, the 5% standard deviation in our measurements of $\langle(\Delta Lk)^2\rangle$ causes a 20% error in the calculated value of C. Our result is in a good agreement with the value of 3.0×10^{-19} erg×cm previously found using this approach (17,19,20). However, lower values of C ($1.7–2.4 \times 10^{-19}$ erg×cm) have been found by other techniques (11,30,48–50).

In pure NaCl solutions, γ decreases monotonically with NaCl concentration. As a result, over the range 0.01–0.2 M NaCl the value of $d\sigma/d$ log[NaCl] equals $–0.0025 \pm 0.0003$. This value is substantially lower than the previously reported value of –0.0045 found by essentially the same technique (39). The reason for this discrepancy may arise from the fact that nearly stoichiometric amounts of topo I have to be used to achieve complete relaxation of DNA. We found only a limited range of enzyme:DNA molar ratios over which the distributions did not depend on topo I concentration. At higher or lower enzyme concentrations both the width and the center of the distribution changed and previous determinations of the salt dependence of σ may have used distributions not quite at equilibrium. Alternatively, because the ranges of NaCl concentration used in this and the previous studies (39) overlap only partially, the discrepancy might reflect a non-linear dependence of γ on log[Na^+]. In good agreement with the previous study (39), we found that if $MgCl_2$ is the only salt present at a concentration higher than 0.5 mM, the DNA helical repeat is practically independent of the salt concentration. In the mixed NaCl/$MgCl_2$ solutions, however, the dependence of γ on $MgCl_2$ concentration becomes increasingly more pronounced as NaCl concentration increases (see Fig. 6). In the presence of $MgCl_2$, the effect of NaCl on the value of γ is opposite to that found for pure NaCl solution, with γ decreasing with increasing NaCl concentration. This switch of the sign of the dependence is easy to understand, because γ is smaller in pure $MgCl_2$ solutions than in pure NaCl solutions. If the NaCl concentration is increased in a solution containing $MgCl_2$, sodium ions gradually substitute for magnesium ions and thus increase γ. The substitution is notable only if the $MgCl_2$ concentration is <~10 mM, because the binding of magnesium is much stronger than the binding of sodium ions. In agreement with Paulsen *et al.* (36), our data show that the binding constant of magnesium is ~2 orders of magnitude higher than the binding constant of sodium ions.

Our results (Fig. 6) do not contradict those obtained by Taylor and Hagerman (30), who found no change in γ over the range 0–0.16 M NaCl in the presence of 1 mM $MgCl_2$. We also found no effect of NaCl on γ for the solutions used in their study, containing 1 mM $MgCl_2$ and 1 mM ATP (data not shown). From the data shown in Figure 6 it is reasonable to expect that at some $MgCl_2$ concentration below 0.5 mM the value of γ will be the same at various NaCl concentrations. Because of binding of Mg^{2+} ions by ATP, the 1 mM $MgCl_2$ plus 1 mM ATP used by Taylor and Hagerman (30) happened to yield such a concentration of free Mg^{2+} ions.

ACKNOWLEDGEMENTS

This work was supported by NIH grants GM31657 to N.R.C. and GM54215 to A.V.V.

REFERENCES

1 Vologodskii,A.V. and Cozzarelli,N.R. (1994) *Annu. Rev. Biophys. Biomol. Struct.*, **23**, 609–643.
2 Bednar,J., Furrer,P., Stasiak,A., Dubochet,J., Egelman,E.H. and Bates,A.D. (1994) *J. Mol. Biol.*, **235**, 825–847.
3 Langowski,J., Kapp,U., Klenin,K. and Vologodskii,A.V. (1994) *Biopolymers*, **34**, 639–646.
4 Boles,T.C., White,J.H. and Cozzarelli,N.R. (1990) *J. Mol. Biol.*, **213**, 931–951.
5 Gebe,J.A., Delrow,J.J., Heath,P.J., Fujimoto,B.S., Stewart,D.W. and Schurr,J.M. (1996) *J. Mol. Biol.*, **262**, 105–128.
6 Klenin,K.V., Vologodskii,A.V., Anshelevich,V.V., Dykhne,A.M. and Frank-Kamenetskii,M.D. (1991) *J. Mol. Biol.*, **217**, 413–419.
7 Frank-Kamenetskii,M.D. (1990) In Cozzarelli,N.R. and Wang,J.C. (eds), *DNA Topology and its Biological Effects*. Cold Spring Harbor Laboratory Press, Cold Spring Harbor, NY, pp. 185–216.
8 Depew,R.E. and Wang,J.C. (1975) *Proc. Natl. Acad. Sci. USA*, **72**, 4275–4279.
9 Pulleyblank,D.E., Shure,M., Tang,D., Vinograd,J. and Vosberg,H.P. (1975) *Proc. Natl. Acad. Sci. USA*, **72**, 4280–4284.
10 Lee,C.H., Mizusawa,H. and Kakefuda,T. (1981) *Proc. Natl. Acad. Sci. USA*, **78**, 2838–2842.
11 Shore,D. and Baldwin,R.L. (1983) *J. Mol. Biol.*, **170**, 983–1007.
12 Horowitz,D.S. and Wang,J.C. (1984) *J. Mol. Biol.*, **173**, 75–91.
13 Duguet,M. (1993) *Nucleic Acids Res.*, **21**, 463–468.
14 Benham,C.J. (1978) *J. Mol. Biol.*, **123**, 361–370.
15 Vologodskii,A.V., Lukashin,A.V., Anshelevich,V.V. and Frank-Kamenetskii,M.D. (1979) *Nucleic Acids Res.*, **6**, 967–982.
16 Le Bret,M. (1980) *Biopolymers*, **19**, 619–637.
17 Frank-Kamenetskii,M.D., Lukashin,A.V., Anshelevich,V.V. and Vologodskii,A.V. (1985) *J. Biomol. Struct. Dynam.*, **2**, 1005–1012.
18 Levene,S.D. and Crothers,D.M. (1986) *J. Mol. Biol.*, **189**, 73–83.
19 Shimada,J. and Yamakawa,H. (1988) *Biopolymers*, **27**, 657–673.
20 Klenin,K.V., Vologodskii,A.V., Anshelevich,V.V., Klisko,V.Y., Dykhne,A.M. and Frank-Kamenetskii,M.D. (1989) *J. Biomol. Struct. Dynam.*, **6**, 707–714.

21 Stigter,D. (1977) *Biopolymers*, **16**, 1435–1448.
22 Vologodskii,A.V. and Cozzarelli,N.R. (1995) *Biopolymers*, **35**, 289–296.
23 Brian,A.A., Frisch,H.L. and Lerman,L.S. (1981) *Biopolymers*, **20**, 1305–1328.
24 Yarmola,E.G., Zarudnaya,M.I. and Lazurkin,Y.S. (1985) *J. Biomol. Struct. Dynam.*, **2**, 981–993.
25 Rybenkov,V.V., Cozzarelli,N.R. and Vologodskii,A.V. (1993) *Proc. Natl. Acad. Sci. USA*, **90**, 5307–5311.
26 Shaw,S.Y. and Wang,J.C. (1993) *Science*, **260**, 533–536.
27 Wasserman,S.A., White,J.H. and Cozzarelli,N.R. (1988) *Nature*, **334**, 448–450.
28 Ausubel,F.M., Brent,R., Kingston,R.E., Moore,D.D., Seidman,J.G., Smith,J.A. and Struhl,K. (eds) (1989) *Current Protocols in Molecular Biology*. Wiley–Interscience, New York, NY.
29 Barzilai,R. (1973) *J. Mol. Biol.*, **74**, 739–742.
30 Taylor,W.H. and Hagerman,P.J. (1990) *J. Mol. Biol.*, **212**, 363–376.
31 Dynan,W.S., Jendrisak,J.J., Hager,D.A. and Burgess,R.R. (1981) *J. Biol. Chem.*, **256**, 5860–5865.
32 Wang,J.C., Peck,L.J. and Becherer,K. (1983) *Cold Spring Harbor Symp. Quant. Biol.*, **47**, 85–91.
33 Klenin,K.V., Vologodskii,A.V., Anshelevich,V.V., Dykhne,A.M. and Frank-Kamenetskii,M.D. (1988) *J. Biomol. Struct. Dynam.*, **5**, 1173–1185.
34 Hagerman,P.J. (1988) *Annu. Rev. Biophys. Biophys. Chem.*, **17**, 265–286.
35 Krasnow,M.A. and Cozzarelli,N.R. (1982) *J. Biol. Chem.*, **257**, 2687–2693.
36 Paulsen,M.D., Anderson,C.F. and Record,M.T.J. (1988) *Biopolymers*, **27**, 1249–1265.
37 Wang,J.C. (1969) *J. Mol. Biol.*, **43**, 25–39.
38 Shure,M. and Vinograd,J. (1976) *Cell*, **8**, 215–226.
39 Anderson,P. and Bauer,W. (1978) *Biochemistry*, **17**, 594–601.
40 Bauer,W.R. (1978) *Annu. Rev. Biophys. Bioengng*, **7**, 287–313.
41 Vologodskii,A.V. (1992) *Topology and Physics of Circular DNA*. CRC Press, Boca Roton, FL.
42 Peck,L.J. and Wang,J.C. (1983) *Proc. Natl. Acad. Sci. USA*, **80**, 6206–6210.
43 Ellison,M.J., Kelleher,R.J., Wang,A.H., Habener,J.F. and Rich,A. (1985) *Proc. Natl. Acad. Sci. USA*, **82**, 8320–8324.
44 Ellison,M.J., Feigon,J., Kelleher,R.J., Wang,A.H., Habener,J.F. and Rich,A. (1986) *Biochemistry*, **25**, 3648–3655.
45 Mirkin,S.M., Lyamichev,V.I., Kumarev,V.P., Kobzev,V.F., Nosikov,V.V. and Vologodskii,A.V. (1987) *J. Biomol. Struct. Dynam.*, **5**, 79–88.
46 Aboul-ela,F., Bowater,R.P. and Lilley,D.M. (1992) *J. Biol. Chem.*, **267**, 1776–1785.
47 Chen,Y. (1981) *J. Chem. Phys.*, **75**, 2447–2453.
48 Thomas,J.C., Allison,S.A., Appelof,C.J. and Schurr,J.M. (1980) *Biophys. Chem.*, **12**, 177–188.
49 Shibata,J.M., Fujimoto,B.S. and Schurr,J.M. (1985) *Biopolymers*, **24**, 1909–1930.
50 Heath,P.J., Clendenning,J.B., Fujimoto,B.S. and Schurr,J.M. (1996) *J. Mol. Biol.*, **260**, 718–730.